Biophysical Journal, Volume 98

Supporting Material

Binding and cleavage of *E. coli* HUβ by the *E. coli* Lon protease

Jiahn-Haur Liao, Yu-Ching Lin, Chiau-Wei Hsu, Alan Yueh-Luen Lee, Tse-An Chen, Chun-Hua Hsu, Jiun-Ly Chir, Kuo-Feng Hua, Tzu-Hua Wu, Li-Jenn Hong, Pei-Wen Yen, Arthur Chiou, and Shih-Hsiung Wu

Supplemental Data

Binding and cleavage of *E. coli* HUβ by the *E. coli* Lon protease

Jiahn-Haur Liao[*,†] , Yu-Ching Lin[‡,†] , Chiau-Wei Hsu[§], Alan Yueh-Luen Lee[¶], Tse-An Chen[‡], Chun-Hua Hsu[‖], Jiun-Ly Chir[*], Kuo-Feng Hua[*], Tzu-Hua Wu[**] Li-Jenn Hong[§], Pei-Wen Yen[§], Arthur Chiou [§,††] , Shih-Hsiung Wu[*,††]

[*]Institute of Biological Chemistry, Academia Sinica, Taipei 115, Taiwan,
[‡] Institute of Biochemical Sciences, National Taiwan University, Taipei 106, Taiwan,
[§]Institute of Biophotonics, National Yang-Ming University, Taipei, Taiwan,
[¶]Department of Biotechnology, Kaohsiung Medical University, Kaohsiung, Taiwan,
[‖]Department of Agricultural Chemistry, National Taiwan University, Taiwan
[**]School of Pharmacy, College of Pharmacy, Taipei Medical University, Taipei 110, Taiwan

Running head: The degradation process of *E. coli* Lon protease

[††]To whom correspondence should be addressed: Shih-Hsiung Wu, Institute of Biological Chemistry, Academia Sinica, Taipei 115, Taiwan, ROC, Tel: 8862 2785 5696, Ext. 7101; Fax: 8862 2653 9142, E-mail: shwu@gate.sinica.edu.tw; Arthur Chiou, Institute of Biophotonics, National Yang-Ming University, Taipei 112, Taiwan, ROC, Tel: 8862 2820 1091; Fax: 8862 2820 1093, E-mail: aechiou@ym.edu.tw

[†] Both contributed equally to this work

Contents:

1. Preparation of Lon and HU

The gene encoding *Bacillus subtilis* HU (*Bs*-HU) was cloned from chromosomal DNA. The genes encoding *Bs*-HU, HUα, and HUβ were amplified using the polymerase chain reaction. The forward primer contained an ATG initiation codon and an *Nde*I restriction site. The reverse primer complementarily overlapped the 3′-end of the coding region and contained an *Xho*I site. After double-digestion with *Nde*I and *Xho*I, the product was purified and ligated into the *Nde*I/*Xho*I sites of the isopropyl β-D-thiogalactoside (IPTG)-inducible *E. coli* expression vector pET21a (+) (Novagen, La Jolla, USA). *E. coli* strain BL21(DE3) was transformed with the recombinant plasmids. The primers A20Q-forward (5′-tctaaagctcaggctggccg-3′), A20Q-reverse (5′-ggccagcctgagctttagag-3′), A20D-forward (5′-atctctaaagctgacgctggccgtgcg-3′), and A20D-reverse (5′-cgcacggccagcgtcagctttagagat-3′) were used to introduce a mutation into *E. coli hupB*. The molecular masses of mutated proteins, HUβ-A20Q and HUβ-A20D, were checked by mass spectroscopy.

Cultures were incubated at 37 °C until they reached an optical density of 0.6 at 600 nm. Expression was induced by the addition of IPTG (1 mM), and cultures were incubated another 4 h. Cells were harvested and resuspended in 50 mM Tris-HCl (pH 8.0), 50 mM NaCl, 10 mM β-mercaptoethanol and lysed by ultrasonication. The lysed cells were centrifuged for 20 min at 20,000×*g* to pellet insoluble debris. The lysate was mixed with Ni-Sepharose 6 fast flow gel (GE Healthcare, Taipei, Taiwan) for 30 min at 4 °C; the mixture was placed in an Econo-Pac column (BioRad Laboratories, USA). The column was washed with buffer containing 50 mM Tris-HCl (pH 8.0), 50 mM NaCl, and 20 mM imidazole. The HU protein was eluted with the same buffer containing 200 mM imidazole.

2. The *E. coli* HUαβ heterodimer is not a substrate of *E. coli* Lon

HUβ is degraded specifically in the absence of HUα (Bonnefoy and others 1989), and HUαβ is the major HU dimer when HUα and HUβ are mixed (Ramstein and others 2003). Whether the heterodimer HUαβ is degraded by *Ec*-Lon was tested by mixing equal amounts of HUα and HUβ together with 6 M urea and incubated at 37 °C for 30 min. Urea was then removed by ultrafiltration. The heterodimer HUαβ was then incubated with *Ec*-Lon at 37 °C for 2 h and then analyzed by SDS-PAGE (Fig. S1). *E. coli* HUαβ was not cleaved by *Ec*-Lon.

3. Cleavage sites of *Ec*-Lon in HUβ

The preference for cleavage after alanine and leucine was reported previously (Maurizi 1987; Nishii and others 2002; Nishii and others 2005; Ondrovicova and others 2005; Van Melderen and others 1996). We also incubated HUα, HUβ, or *Bs*-HU with *Bt*-Lon in the presence of ATP for 10 min and analyzed the peptide fragments (Table S2). We found 18, 20, and 12 peptide fragments of HUα, HUβ, and *Bs*-HU, respectively. All of the amino acids of sites P1 and P1' of the cleavage sites of *Ec*-Lon and *Bt*-Lon yielding the peptide fragments are identified and the cleavage frequency of each site is listed in Table S2.

When HUβ was used as the substrate for both *Ec*-Lon and *Bt*-Lon, the preferred cleavage sites were A–A (P1–P1') and L–K. The preferred cleavage sites of *Bt*-Lon in HUα were L–V, L–S, A–I, and A–K, and in *Bs*-HU the preferred cleavage sites of *Bt*-Lon were A–T and L–I. Therefore, both *Ec*-Lon and *Bt*-Lon preferentially cleave at

the C-terminus of alanine or leucine. For example, when *E. coli* HUβ was used as the substrate for *Ec*-Lon, cleavage occurred at the C-terminus of alanine and leucine at 7 and 6 times, respectively, out of 17. When *Bt*-Lon cleaved the various HU proteins, of a total of 93 cleavages, 41 and 27 occurred at the C-terminus of alanine and leucine, respectively (Table S2).

4. The main cleavage site of *Ec*-Lon in HUβ

Based on amino acid sequence comparisons of the three HU proteins (HUα, HUβ, and *Bs*-Hu) and previous results, we decided to construct a HUβ protein with a mutation in residue 20, HUβ-A20Q, to investigate the cleavage site of *Ec*-Lon in more detail. SDS-PAGE analysis showed that HUβ was completely digested after 7 h of incubation with *Ec*-Lon and ATP (4.2 μM), whereas the same concentration of the mutant protein HUβ-A20Q was degraded only to a small extent (Fig. S4). Similar results were obtained when different concentrations of HUβ and HUβ-A20Q were used (data not shown). The minor bands seen in Fig. S2 are the autodegradation products of the Lon protease (Vasilyeva and others 2002); autodegradation occurred spontaneously during longer incubations and was prevented by ATP. Therefore, the minor bands are not contaminating proteins. These results indicate that the A20Q mutation reduces the degradation rate of HUβ by *Ec*-Lon.

5. Optical tweezers set-up

The optical tweezers set-up is shown in Fig. S5. A quadrant photodiode (QPD, S7479, Hamamatsu) is a set of four silicon photodiodes that provide an analog voltage output directly proportional to the light spot position on the detector active area. A

QPD package with a 5 × 5mm active area and with a 0.03 mm gap between each photodiode was used to detect the position of the beads coated with proteins. A notch filter was used to block the trapping beam (λ = 1064 nm) from entering the QPD. The electrical output signals from the QPD were recorded by a data acquisition system (DAQ) for data analysis. Wide-field images of the trapped bead were captured by a CCD camera (WAT-120N, Watec) for optical alignment of the trap and for monitoring and image analysis of the trapped bead. The field of view of the CCD camera was calibrated by a Ronchi ruling (5,000 lines $inch^{-1}$) to be approximately 38.99 μm × 29.47 μm (0.06 μm $pixel^{-1}$).

6. Optical spring constant measurement

We tracked the Brownian motion of a trapped 2.88 μm polystyrene bead (suspended in PBS buffer solution) with a 1064 nm laser beam (ND: YVO_4, 2 mW) and analyzed its position. We used Boltzmann statistics to calculate the optical force field E(x), which is represented by the parabolic potential with optical spring constants k_x. The optical force field can be represented by the parabolic potential, and we defined the optical spring constants on the transverse plane in the optical tweezers using the following equations (E-L. Florin 1998):

$$\rho(x)\,dx = Ce^{-E(x)/K_BT} \qquad \text{(Eq. 1)}$$

and

$$E(x) = -K_BT \ln \rho(x) + K_BT \ln C = \frac{1}{2}\left(k_{OT}x^2\right) \qquad \text{(Eq. 2)}$$

where K_B is the Boltzmann constant, ρ(x) is the probability function of the particle position along the x-axis, C is the normalization constant, E(x) is the potential energy function along the x-axis, and k_{OT} is the optical spring constant (or force constant) along the x-axis. By fitting the experimental data ρ(x) with Eq. 2, the optical spring

constant along the x-axis was determined to be 115±1 pN μm^{-1} when the trapping optical power was approximately 19 mW.

7. Proteins immobilized on polystyrene beads

Adsorption of trypsin to a polystyrene surface is almost irreversible with respect to dilution, whereas trypsin on a silica gel surface is easily desorbed (Koutsopoulos and others 2007). We therefore chose hydrophobic polystyrene beads as the solid supporting material for protein immobilization. However, trypsin coating a polystyrene surface is not active (Koutsopoulos and others 2007), but a hyperthermostable enzyme is active (Koutsopoulos and others 2004).

We incubated the polystyrene beads overnight with Lon or a HU protein. The bare regions of the beads were then coated with BSA. Both the coated and the uncoated beads were examined by scanning electron microscopy (Fig. S6). The surface of the beads became coarse when coated with proteins.

Polystyrene beads (10 μl) were washed with buffer containing 25 mM Tris-HCl (pH 8.0), 75 mM NaCl, 5 mM $MgCl_2$, 5 mM $CaCl_2$, and 10 % glycerol. Large polystyrene beads (12.3 μm in diameter) were incubated with Lon protease at 4 °C for 18 h. After incubation, the beads were washed with 1 ml of the same buffer. After wash, the Lon-coated beads were suspended in 100 μl buffer, and then 30 μl beads were used in activity assays. The Lon protease coated on the polystyrene beads remained active (Fig. S7), but the activity was lower than that of Lon (~4 μg) in solution. However, the exact amount of protein coating the beads is unknown.

8. Rupture force measurements

The rupture force measurements are illustrated in Fig. S8. Three observations were made during the force measurements (Fig. S9):

(1) The small bead stayed in the vicinity of the trapping beam axis independent of the position of the larger bead, which indicated that the two beads did not bind to each other (Fig. S9A). This could happen when the point of contact was in a region where there was no protein (or a trace amount of protein) on either one or both beads.

(2) The small bead stuck to the large bead and followed the displacement of the large bead until it escaped from the optical trap, which indicated that the interaction force (or adherence force owing to protein-protein binding) was larger than the maximum optical force. This could happen when the point of contact was in a region with an excessive amount of proteins on both beads. In this case, the optical force could not overcome the binding force and the rupture force could not be measured (Fig. S9B). In Fig. S6B, the decrease in the signal on the right side of the figure was caused by the laser spot (of the tracking beam) on the QPD escaping the sensing area of the QPD.

(3) The small bead was pulled away from the beam axis by the large bead up to the point when the optical force overcame the protein–protein binding force; at the threshold point, the binding was broken, and the small bead bounced back to the equilibrium position on the beam axis. In this case, the maximum optical force at the breaking threshold was defined as the rupture force (Fig. S9C).

The number of measurements that fell into these three cases is summarized in Table S3. Experiments with BSA-coated beads always fell in case (1), which indicated that there was no interaction between BSA and the Hu proteins.

9. Discussion

Substrate recognition and cleavage specificity are distinctly different phenomena for chaperone-protease complexes such as Lon. The former is dependent on elements

in the chaperone that bind substrate proteins in preparation for unfolding and translocating them to the protease domain. The latter refers to the way in which polypeptides fit into the proteolytic active site of Lon and has more to do with the peptide products generated than with the proteins selected for degradation.

10. References

Bonnefoy E, Almeida A, Rouviere-Yaniv J. 1989. Lon-dependent regulation of the DNA binding protein HU in Escherichia coli. Proc Natl Acad Sci U S A 86(20):7691-5.

E-L. Florin AP, E. H. K. Stelzer, and J. K. H. Horber. . 1998. Applied Physics A 66:75-78.

Koutsopoulos S, Patzsch K, Bosker WT, Norde W. 2007. Adsorption of trypsin on hydrophilic and hydrophobic surfaces. Langmuir 23(4):2000-6.

Koutsopoulos S, van der Oost J, Norde W. 2004. Adsorption of an endoglucanase from the hyperthermophilic Pyrococcus furiosus on hydrophobic (polystyrene) and hydrophilic (silica) surfaces increases protein heat stability. Langmuir 20(15):6401-6.

Maurizi MR. 1987. Degradation in vitro of bacteriophage lambda N protein by Lon protease from Escherichia coli. J Biol Chem 262(6):2696-703.

Nishii W, Maruyama T, Matsuoka R, Muramatsu T, Takahashi K. 2002. The unique sites in SulA protein preferentially cleaved by ATP-dependent Lon protease from Escherichia coli. Eur J Biochem 269(2):451-7.

Nishii W, Suzuki T, Nakada M, Kim YT, Muramatsu T, Takahashi K. 2005. Cleavage mechanism of ATP-dependent Lon protease toward ribosomal S2 protein.

FEBS Lett 579(30):6846-50.

Ondrovicova G, Liu T, Singh K, Tian B, Li H, Gakh O, Perecko D, Janata J, Granot Z, Orly J and others. 2005. Cleavage site selection within a folded substrate by the ATP-dependent lon protease. J Biol Chem 280(26):25103-10.

Ramstein J, Hervouet N, Coste F, Zelwer C, Oberto J, Castaing B. 2003. Evidence of a thermal unfolding dimeric intermediate for the Escherichia coli histone-like HU proteins: thermodynamics and structure. J Mol Biol 331(1):101-21.

Van Melderen L, Thi MH, Lecchi P, Gottesman S, Couturier M, Maurizi MR. 1996. ATP-dependent degradation of CcdA by Lon protease. Effects of secondary structure and heterologous subunit interactions. J Biol Chem 271(44):27730-8.

Vasilyeva OV, Kolygo KB, Leonova YF, Potapenko NA, Ovchinnikova TV. 2002. Domain structure and ATP-induced conformational changes in Escherichia coli protease Lon revealed by limited proteolysis and autolysis. FEBS Lett 526(1-3):66-70.

11. Table

Table S1. Peptide fragments with a Mowse score >25 detected after incubation of *Ec*-Lon with HUβ and ATP for 5, 10, and 30 min. The residues flanking the peptide fragment detection are set apart from the fragment with hyphens. ●**:** peptide fragments detected.

Peptide	Residues	Peptide fragment	Reaction time (min)		
			30	10	5
1	21 – 30	A-AGRALDAIIA-S	●	●	
2	37 – 47	L-KEGDDVALVGF-G	●		●
3	20 – 32	A-AAGRALDAIIASV-T	●		
4	45 – 57	L-VGFGTFAVKERAA-R	●	●	
5	37 – 50	L-KEGDDVALVGFGTF-A	●	●	
6	23 – 36	G-RALDAIIASVTESL-K	●		
7	21 – 33	A-AGRALDAIIASVT-E			●
8	22 – 36	A-GRALDAIIASVTESL-K	●		
9	21 – 36	A-AGRALDAIIASVTESL-K	●	●	●
10	37 – 52	L-KEGDDVALVGFGTFAV-K	●	●	
11	20 – 36	A-AAGRALDAIIASVTESL-K	●		
12	12 – 32	A-AGADISKAAAGRALDAIIASV-T	●	●	
13	1 – 19	MNKSQLIDKIAAGADISKA-A	●		
14	12 – 33	A-AGADISKAAAGRALDAIIASVT-E	●		
15	1 – 18	MNKSQLIDKIAAGADISK-A		●	
16	1 – 20	MNKSQLIDKIAAGADISKAA-A	●		
17	23 – 44	G-RALDAIIASVTESLKEGDDVAL-V	●		
18	12 – 36	A-AGADISKAAAGRALDAIIASVTESL-K	●		
19	21 – 44	A-AGRALDAIIASVTESLKEGDDVAL-V	●		
20	21 – 47	A-AGRALDAIIASVTESLKEGDDVALVGF-G	●	●	
21	1 – 30	MNKSQLIDKIAAGADISKAAAGRALDAIIA-S	●	●	
22	12 – 47	A-AGADISKAAAGRALDAIIASVTESLKEGDDVALVGF-G	●		
23	1 – 36	MNKSQLIDKIAAGADISKAAAGRALDAIIASVTESL-K	●		

Table S2. The P1-P1' site of every peptide fragment was listed in this table. Every peptide fragment has at least one enzyme cutting site. The same cutting site may be counted more than once time, because one cutting site created two peptide fragments. Frequencies of the cutting sites at 10 min were listed in the following table.

Enzyme	*Ec*-Lon		*Bt*-Lon		*Bt*-Lon		*Bt*-Lon	
Substrate	HUβ		HUβ		HUα		*Bs*-HU	
Cleavage site	P1-P1'	Frequency	P1-P1'	Frequency	P1-P1'	Frequency	P1-P1'	Frequency
	A-A	4	A-A	14	A-A	2	A-L	2
	A-R	1	A-G	1	A-I	4	A-R	1
	A-S	1	A-R	1	A-K	4	A-S	1
	F-A	1	A-S	2	A-N	1	A-T	5
	F-G	1	F-G	3	F-G	2	A-V	3
	G-R	1	G-F	1	G-F	1	F-G	1
	K-A	1	G-R	1	K-A	1	L-D	3
	L-K	3	K-A	1	L-A	2	L-I	5
	L-V	1	L-K	4	L-I	1	T-K	1
	V-K	1	L-V	2	L-K	1	V-D	1
	V-T	1	S-L	1	L-S	4		
			T-E	3	L-V	5		
			V-G	1	N-H	1		
			V-T	3	T-E	1		
					T-Q	1		
					V-N	1		
Total		16		38		32		23

Table S3. Rupture force measurements. The number of measurements that fell into the three cases described in the text and in Fig. S6 obtained with the proteins listed are indicated.

Buffer without ATP

	Number of cases or experiments			
Protein	(3) Rupture force measurements	(2) Sticky binding	(1) No interaction	Total
HUα	13	18	58	71
HUβ	14	23	46	83
HUβ-A20D	9	6	43	58
BSA	0	0	15	15

Buffer with ATP

	Number of cases or experiments			
Protein	(3) Rupture force measurements	(2) Sticky binding	(1) No interaction	Total
HUα	13	15	45	73
HUβ	12	11	48	71
HUβ-A20D	6	10	32	53
BSA	0	0	18	18

12. Figure legends

Fig S1. Testing of the heterodimer HUαβ as a substrate of *Ec*-Lon. HUαβ (0.08 mg ml^{-1}) was incubated with *Ec*-Lon (0.099 mg ml^{-1}) and ATP (5 μM) at 37 °C for 2 h. M: size markers (94, 66, 45, 30, 20, and 14 kDa). Lane 1: HUαβ only; lane 2: HUαβ incubated with *Ec*-Lon and ATP.

Fig. S2. Analyisis of the substrates of the *E. coli* and *Br. thermoruber* Lon proteases by SDS-PAGE. *E. coli* HUα, *E. coli* HUβ, and *Bs*-HU were tested as substrates. Lanes 1–4: incubation for 0, 1, 2, and 3 h in the presence of 5 μM ATP. M: size markers (94, 66, 45, 30, 20, and 14 kDa). (A) *Ec*-Lon and *E. coli* HUβ, (B) *Ec*-Lon and *E. coli* HUα, (C) *Ec*-Lon and *Bs*-HU, (D) *Bt*-Lon and *E. coli* HUβ, (E) *Bt*-Lon and *E. coli* HUα, (F) *Bt*-Lon and *Bs*-HU.

Fig. S3. LC-MS/MS analysis of the peptide fragments of the main peptide formed from *E. coli* HUβ after digestion with the *E. coli* Lon protease for 30 min. The peptide mixture formed after digestion was separated by liquid chromatography-mass spectrometry. The main peptide fragment at 793.87, 2+ (AGRALDAIIASVTESL, MW: 1585.80) was analyzed by a second mass spectroscopy, and this spectrum is shown. The fragment ions 1*, 2*, 3*, 4*, and 5* correlate to AGRALD*, AGRALDA*, AGRALDAI*, AGRALDAII*, and AGRALDAIIA*, respectively.

Fig. S4. Importance of residue 20 in the cleavage of HUβ by Lon. (A) HUβ-A20Q (10,348 Da) (0.078 mg ml^{-1}) and HUβ (0.077 mg ml^{-1}) were each incubated with *Ec*-Lon (0.097 mg ml^{-1}) with or without ATP (4.2 μM) for 7 h. Samples were then denatured by heating and analyzed by SDS-PAGE. M: Size markers (94, 66, 45, 30,

20, and 14 kDa). Lanes: 1, HUβ; 2, *Ec*-Lon and HUβ without ATP; 3, *Ec*-Lon and HUβ with ATP; 4, HUβ-A20Q; 5, *Ec*-Lon and HUβ-A20Q without ATP; 6, *Ec*-Lon and HUβ-A20Q with ATP. Amounts loaded: HUβ (1.93 μg), HUβ-A20Q (1.95 μg), and *Ec*-Lon (2.43 μg). (B) The bands of HUβ and HUβ-A20D were analyzed by IQuant software (Molecular. Dynamics).

Fig. S5. Optical tweezers set-up. A linearly polarized laser beam (λ = 1064 nm, 300 mW, Nd: YVO_4, cw laser) was used for optical trapping. A second laser beam (λ = 632.8 nm, 10 mW, He-Ne cw laser) was used to track the position of the trapped bead.

Fig. S6A–B. Protein-coated polystyrene beads**.** Scanning electron microscopy images of uncoated (A) and Lon-coated (B) polystyrene beads (5000× magnification).

Fig. S7A-C. Protease, peptidase, and ATPase activities of Lon absorbed to the beads. (A) Protease activity of Lon-coated polystyrene beads compared to that of soluble Lon (~4 μg) and a control of beads lacking enzyme. (B) Peptidase activity of Lon-coated polystyrene beads compared to that of soluble Lon (~4 μg) and a control of beads lacking enzyme. (C) ATPase activity of Lon-coated polystyrene beads compared to that of soluble Lon (~4 μg) and a control of beads lacking enzyme.

Fig. S8. Rupture force measurements. (A) The Lon-coated polystyrene bead was moved toward the HU-coated bead. When these two beads touched, the PZT was stopped for 3 min. (B) The Lon-coated polystyrene bead was moved away from the HU-coated bead. (C) Two beads detached and the HU-coated bead returned to the center of the tweezers. (D) A conceptual force vs. position plot of rupture force measurement illustrates the three stages (A, B, and C) described above.

Fig. S9. The three observations made during the rupture force measurements. (A) No interaction between the beads. (B) Sticky binding between the beads. (C) The optical force overcame the protein–protein binding force; at the threshold point the binding was broken, and the maximum optical force at the breaking threshold was defined as the rupture force. See supplementary text for details.

Fig. S10. Pull down assay of protein-coated beads. The Lon-coated beads were soaked in HUβ solution and then washed with buffer. The beads were suspended in SDS-PAGE sample buffer, loaded into wells of gel, and then analysed by SDS-PAGE. Beads with HUβ were soaked in Lon solution and analysed by similar mothods. M: size markers (116, 66, 45, 35, 25, 18 and 14 kDa). Lane 1: Lon-coated beads. Lane 2: HUβ-coated beads.

Fig. S11. BSA is not degraded by Lon protease. M: size markers; Lanes 1–4: BSA was incubated with Lon and ATP for 0, 1, 2, and 3 h, respectively. Lanes 5–8: α-casein was incubated with Lon and ATP for 0, 1, 2, and 3 h, respectively.

Fig. S12. Proposed proteolysis mechanism of Lon protease. We proposed that the cleavage may lead Lon protease conformational change, release products, and then fold back to the state before ATP hydrolysis. However, if cleavage would not occur, then may lead the binding of substrate interfered or competed by other non-substrate molecules. The protein molecules with unfavorable sequence may enter the binding site in the weaker binding state, but not allow to be hydrolyzed and finally release

easily from Lon protease which folds back to the state before ATP hydrolysis.. E: enzyme; S: substrate; non-S: non-substrate.

Fig. S13. Analyisis of the degradation of *E. coli* HUβ by *E. coli* Lon protease in the presence or absence of ATP. Lanes 1–4: incubation for 0, 1, 2, and 3 h in the presence of 5 μM ATP. Lanes 5-7: incubation for 1, 2, and 3 h in the absence of ATP.

13. Figures

Fig. S1.

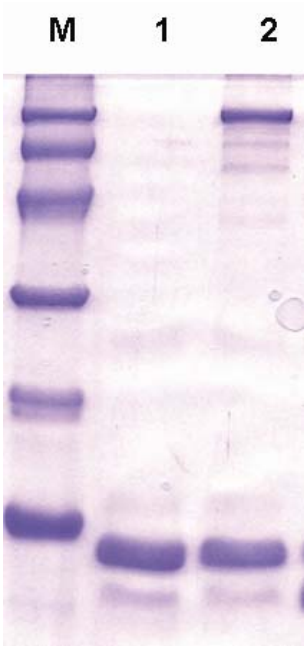

Fig. S2.

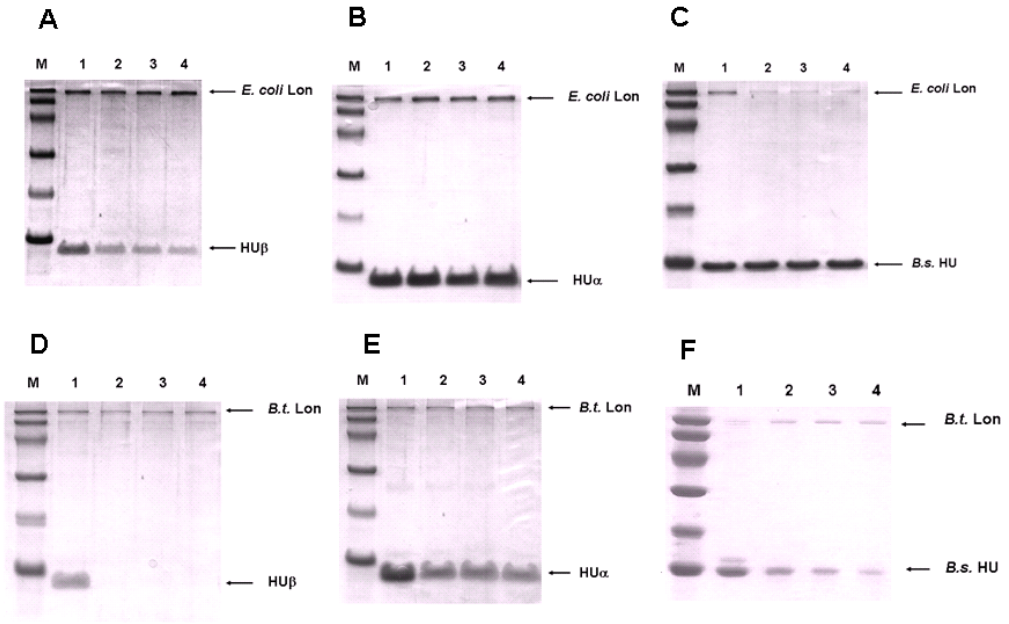
A
M 1 2 3 4
E. coli Lon
HUβ
B
M 1 2 3 4
E. coli Lon
HUα
C
M 1 2 3 4
E. coli Lon
B.s. HU
D
M 1 2 3 4
B.t. Lon
HUβ
E
M 1 2 3 4
B.t. Lon
HUα
F
M 1 2 3 4
B.t. Lon
B.s. HU

Fig. S3.

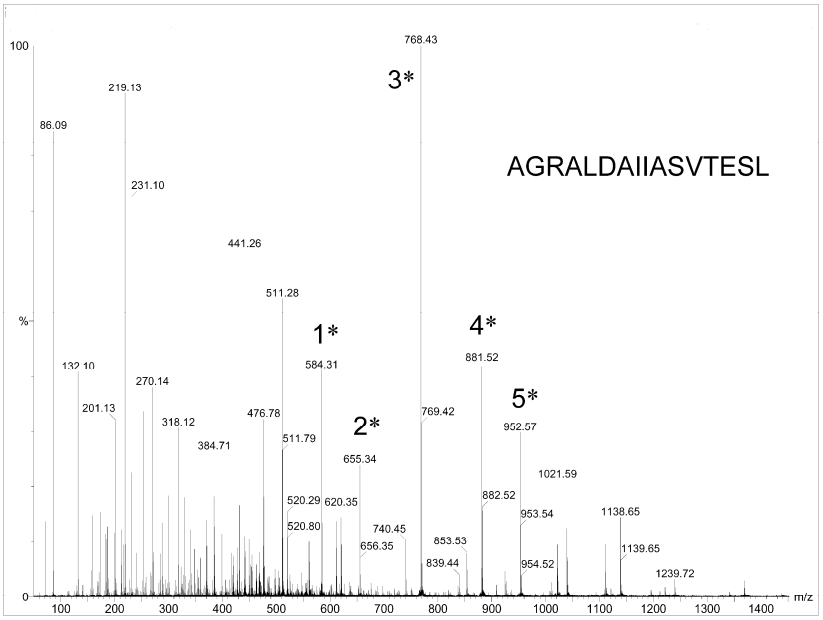
AGRALDAIIASVTESL
768.43
3*
219.13
86.09
231.10
441.26
511.28
1*
4*
584.31
881.52
5*
270.14
201.13
476.78
769.42
318.12
2*
384.71
511.79
655.34
1021.59
520.29
620.35
882.52
953.54
1138.65
520.80
740.45
656.35
839.44
954.52
1139.65
1239.72
100
%
0
m/z
100
200
300
400
500
600
700
800
900
1000
1100
1200
1300
1400

Fig. S4.

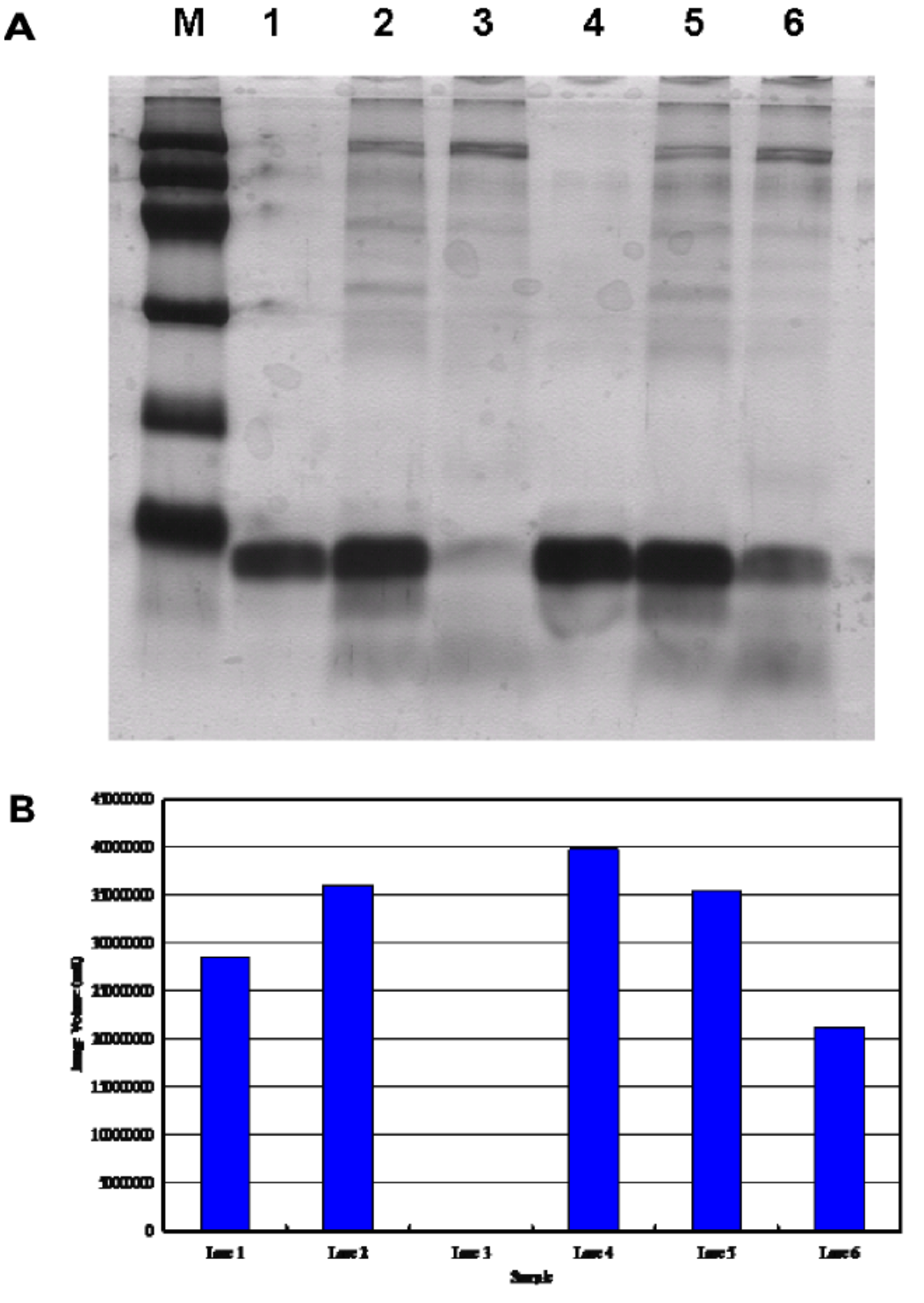

Fig. S5.

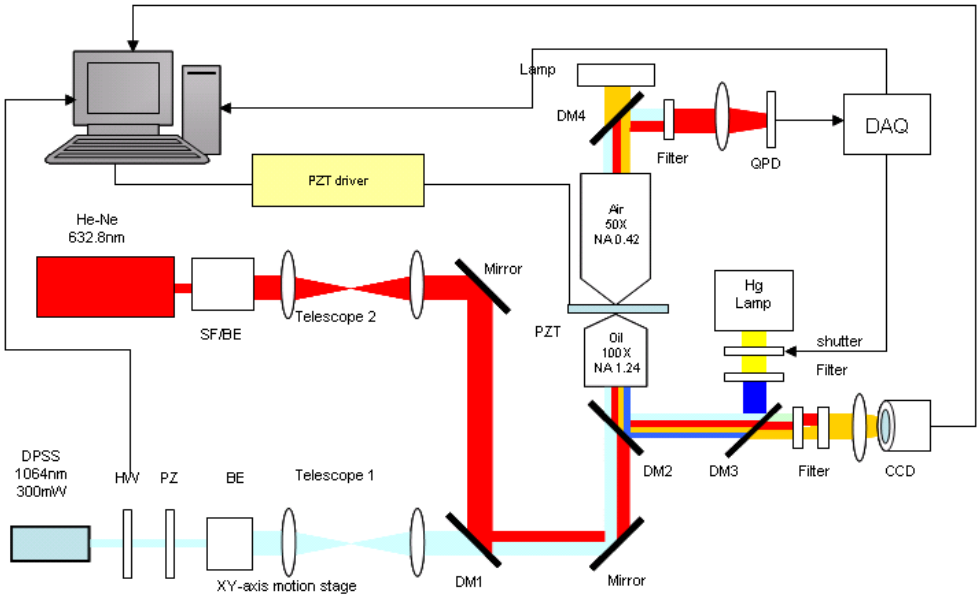
Lamp
DM4
Filter
QPD
DAQ
PZT driver
He-Ne
632.8nm
Air
50X
NA 0.42
Mirror
SF/BE
Telescope 2
PZT
Oil
100X
NA 1.24
Hg
Lamp
shutter
Filter
DPSS
1064nm
300mW
HW
PZ
BE
Telescope 1
DM2
DM3
Filter
CCD
XY-axis motion stage
DM1
Mirror

Fig. S6.

A

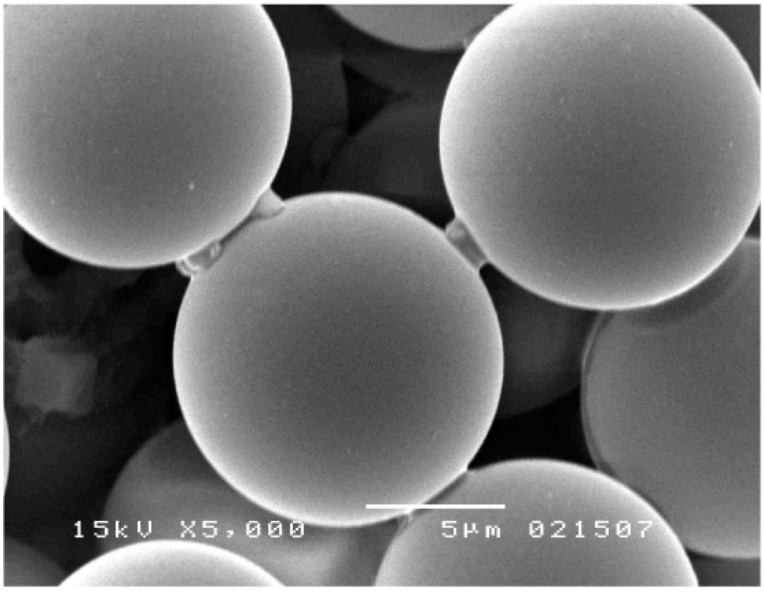

B

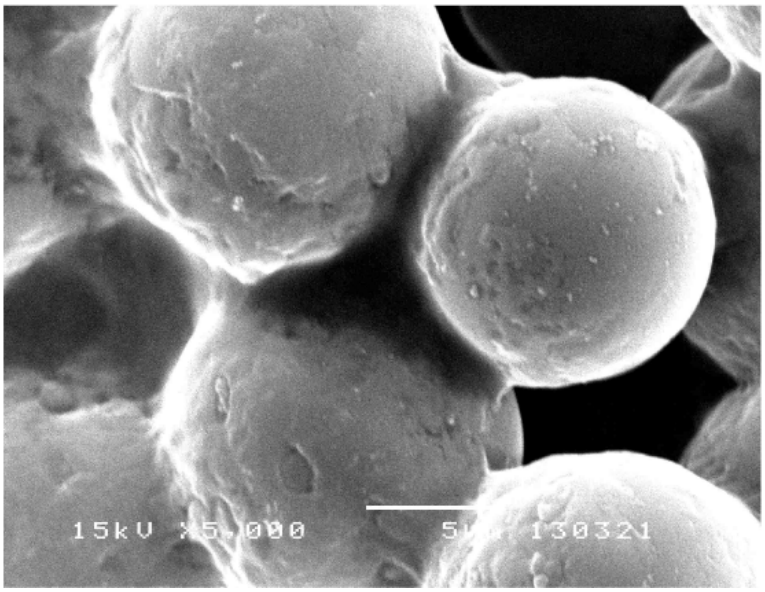

Fig. S7.

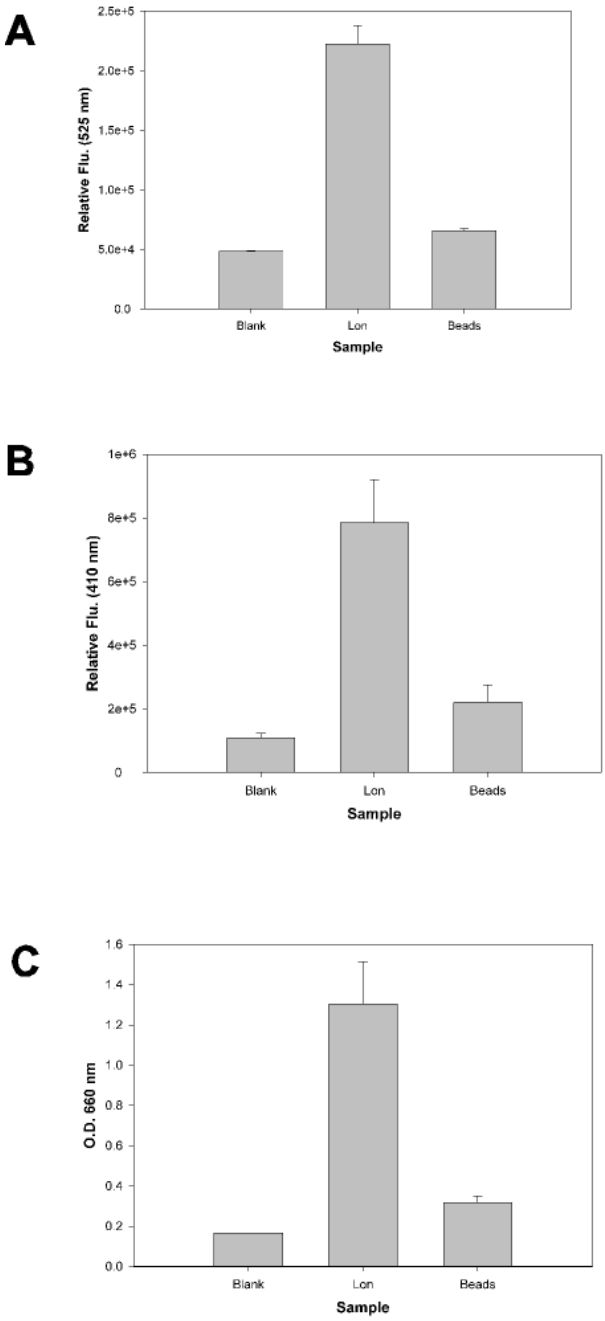
A
2.5e+5
2.0e+5
1.5e+5
1.0e+5
5.0e+4
0.0
Relative Flu. (525 nm)
Blank
Lon
Beads
Sample
B
1e+6
8e+5
6e+5
4e+5
2e+5
0
Relative Flu. (410 nm)
Blank
Lon
Beads
Sample
C
1.6
1.4
1.2
1.0
0.8
0.6
0.4
0.2
0.0
O.D. 660 nm
Blank
Lon
Beads
Sample

Fig. S8.

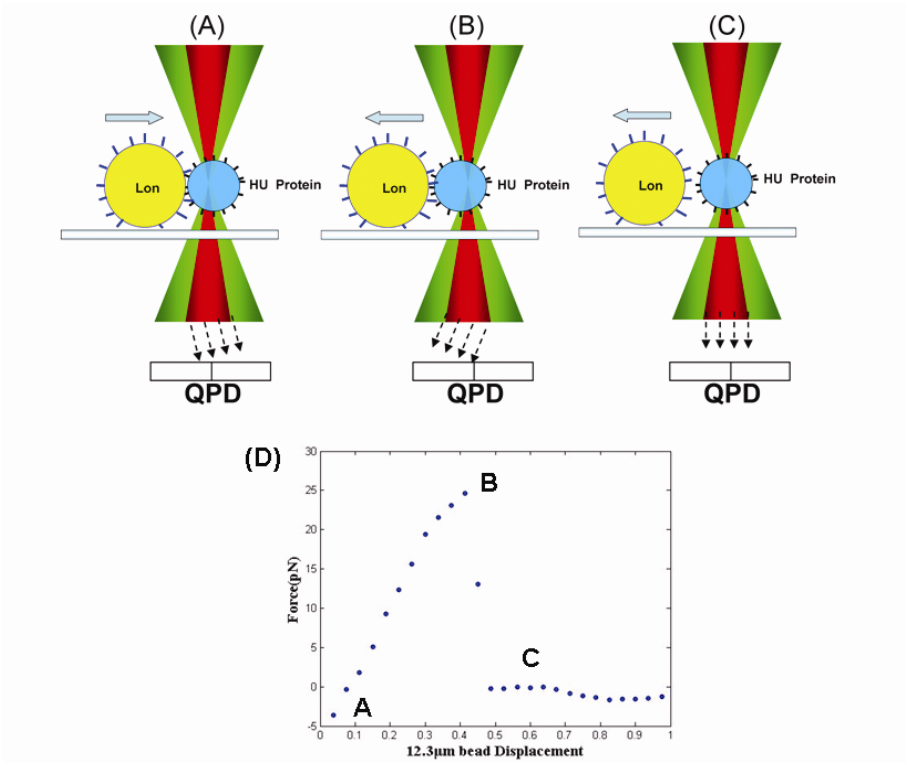
(A)
(B)
(C)
Lon
HU Protein
QPD
(D)
Force(pN)
12.3μm bead Displacement
A
B
C

Fig. S9.

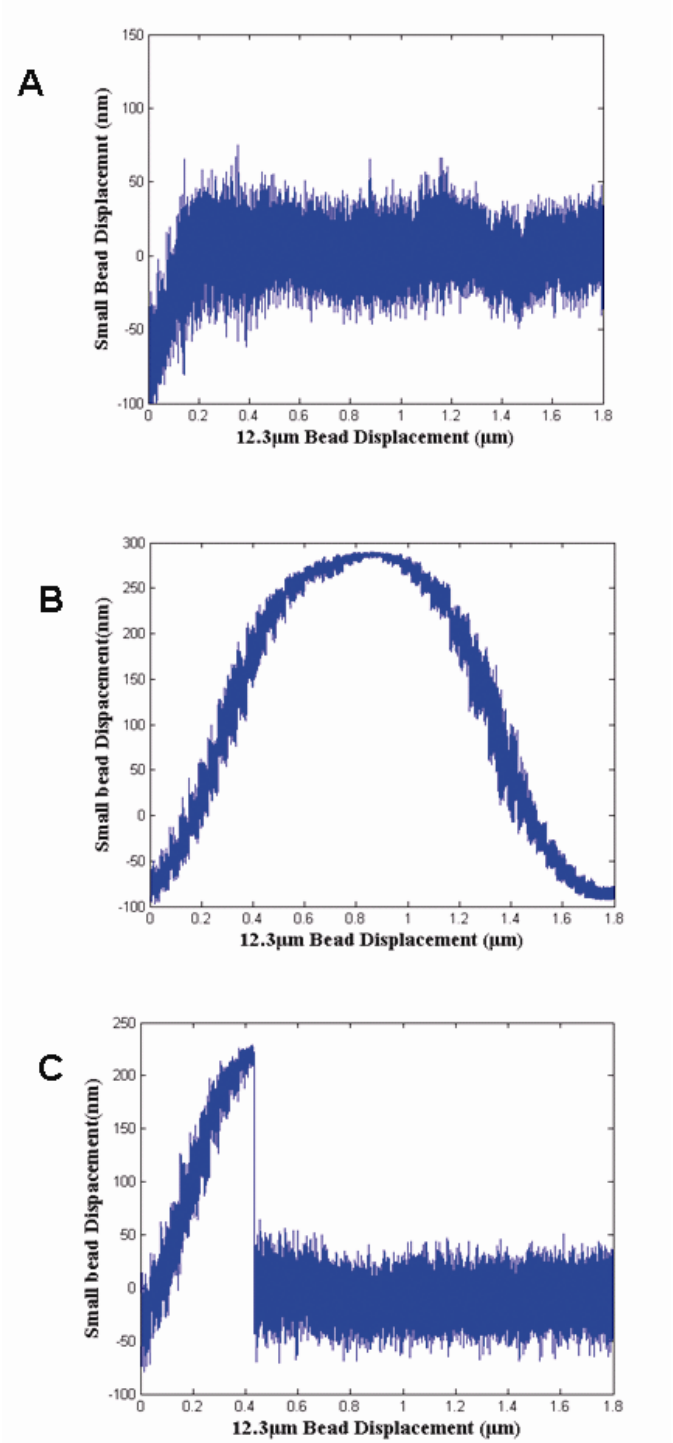
A
Small Bead Displacemnt (nm)
12.3µm Bead Displacement (µm)
B
Small bead Dispacement(nm)
12.3µm Bead Displacement (µm)
C
Small bead Dispacement(nm)
12.3µm Bead Displacement (µm)

Fig. S10.

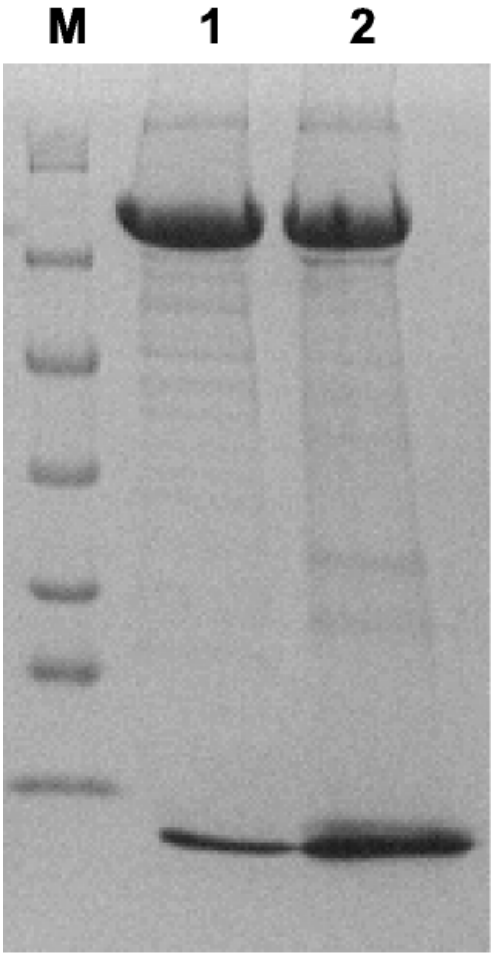

Fig. S11.

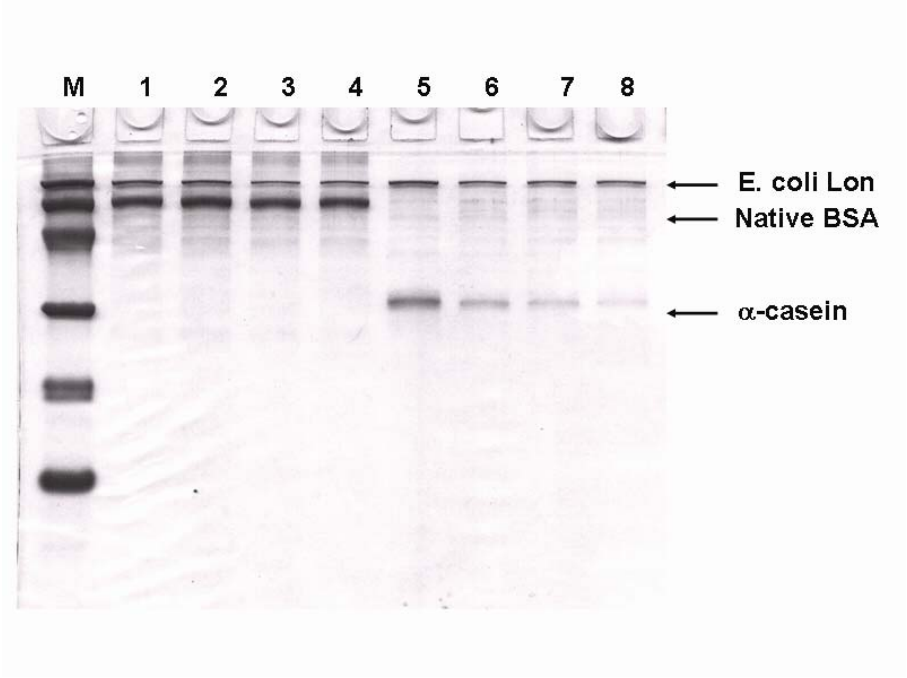

Fig. S12

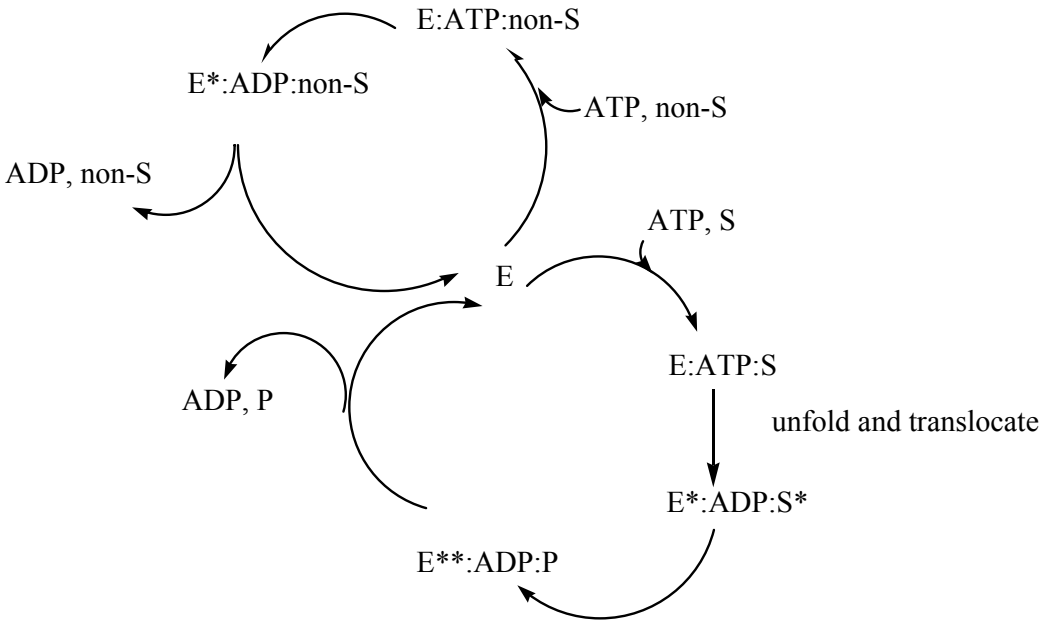
E:ATP:non-S
E*:ADP:non-S
ATP, non-S
ADP, non-S
ATP, S
E
E:ATP:S
ADP, P
unfold and translocate
E*:ADP:S*
E**:ADP:P

Fig. S13